International Journal of Electrical, Electronic and Communication Sciences
ISSN: 2517-9438
Vol:12, No:12, 2018

Map Matching Performance under Various Similarity Metrics for Heterogeneous Robot Teams

M. C. Akay, A. Aybakan, H. Temeltas

Abstract**—**Aerial and ground robots have various advantages of usage in different missions. Aerial robots can move quickly and get a different sight of view of the area, but those vehicles cannot carry heavy payloads. On the other hand, unmanned ground vehicles (UGVs) are slow moving vehicles, since those can carry heavier payloads than unmanned aerial vehicles (UAVs). In this context, we investigate the performances of various Similarity Metrics to provide a common map for Heterogeneous Robot Team (HRT) in complex environments. Within the usage of Lidar Odometry and Octree Mapping technique, the local 3D maps of the environment are gathered. In order to obtain a common map for HRT, informative theoretic similarity metrics are exploited. All types of these similarity metrics gave adequate as allowable simulation time and accurate results that can be used in different types of applications. For the heterogeneous multi robot team, those methods can be used to match different types of maps.

Keywords**—**Common maps, heterogeneous robot team, map matching, informative theoretic similarity metrics.

I. Introduction

MOBILE robot navigation comprises distinctive technologies and applications. In the last few years, there has been an increased use of robotics for navigation. UAVs, UGVs, and unmanned marine vehicles are being used in several applications such as searching, rescuing, exploration, surveillance and reconnaissance. Accomplishing these missions in more efficient ways in the manner of time, energy and accuracy is hard to do with only one robot. Hence, the use of multi robot teams to get ahead those criteria are common. However, this employment for those missions may contain simultaneous actions such as providing coordination and interaction between robots. Moreover, this type of applications breaks new ground challenging problems such as combining bird-eye view images, point clouds, scenes, and etc. with different view ones.

In this work, we are seeking to merge views, collected from VLP-16 Lidar mounted vehicles, by exploiting different types of similarity metrics.

The HRT applications that are popular recently can be grouped by different point of views. For the navigation problem, [1] has a cooperative solution; however, it is only ground robots with various sensors providing alternative capabilities. Also in [2], a parent robot has its ability to operate child robots near its neighborhood and collect data from those in order to gather images of the environment. Further, parent robot knows the relative positions of the child robots and all the robots are ground vehicles. In addition to those, the GPS and IMU information is known and it is quite easy to achieve a detailed map in [3]; however, the purpose is cooperative localization of robots.

In literature, when it comes to provide heterogeneity on robots by defining their ability to move on the ground and in the air, there are also many examples. In one of them [4], it is not desired to merge different types of maps, since common communication interfaces, detection, tracking and etc. is investigated. Moreover, map merging is executed by checking common landmarks inside the environment in [5] where, both agents equipped with laser sensor and camera in order to explore their surroundings. In [6], map merging is handled with looking for occupancy state of the grids.

Similar to our study, in [7] HRT with UAV and UGV have single downward-looking camera and Kinect sensor, respectively. In [8], Visual Odometry (VO) and Monte-Carlo Localization is exploited to obtain local maps of the vehicles. Besides, alignment of the ground and aerial maps is provided by minimum Zero Mean Sum of Squared Differences (ZMSSD) of heights and relative pose. Related to that study, Kaslin et al. use various types of difference metrics in order to align maps [9]. However, we are seeking to find different metrics to align maps by performing similarity metrics of Shannon's Entropies which are defined in [10]. Also, Lidar Odometry [11] and Octree Mapping techniques are exploited in [12] to realize the environment of the agents.

This paper is outlined as follows. In Section II, the definition of problem in map matching for HRT is explained. After that, Section III explains the solution method which involves georeferencing, grid mapping and similarity metrics used to overcome the problem. Finally, simulations done by using the methods in Section III are given in Section IV.

II. Problem Definition

Localization and mapping with heterogeneous team requires detailed studies more than it seems. Separately obtained ground robot and aerial robot maps are needed to be merged in order to define relative positions of the vehicles.

In collaborative mission, UAV gets the aerial base map of the area; also ground robot acquires the draft map. Firstly, attained maps for each vehicle are transformed to height map in order to match those. After that, using similarity metrics, similarities between those to map are computed. Finally, finding the best similarity is executed to obtain the most accurate map of the environment. Block diagram of those

Akay M. C. (MSc.), Aybakan A., and Temeltas H. (Prof Dr.) are with the Control and Automation Engineering Department, Istanbul Technical University, 34469 Istanbul, Turkey (phone: 00902122853030; fax: 0090(212)2852910; e-mail: akaymeh@itu.edu.tr, aybakana@itu.edu.tr, temeltash@itu.edu.tr).

processes can be seen in Fig. 1.

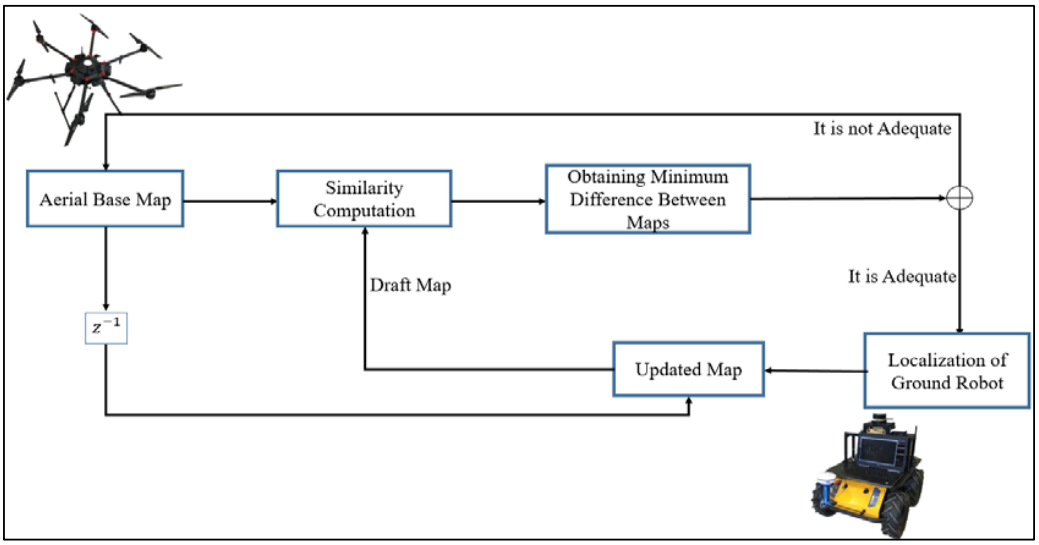

Fig. 1 Block diagram of the common map obtaining process

III. Solution Method

In Lidar mounted vehicle applications, points must be assigned to the global coordinate frames to get static map of the area. Without doing assignment of the points, some laser measurements will be attached to the same point and the map of the area will seem unrecognizable. First of all, both agents need to obtain georeferenced point cloud. Later, georeferenced point cloud is transformed to grid map with the heights of the sensed objects on the cells. After that, heights of the grids are exploited in order to calculate similarities of the areas obtained from both agent's maps.

A. Georeferencing

In our study, point clouds are referenced by using Lidar Odometry method [11]. This method employs only Lidar point cloud data to obtain location information and georeferenced map without any GPS or IMU need.

VLP-16 Lidar has 16 optical scanning unit and those units turn 3000rpm speed. Also, channels scan ±15° of its environment from the unit's vertical center point. Optical channels are shown by $k, k \in \mathbb{Z}^+$, and the map obtained by each channel can be shown by N_k. Let L be the coordinate system of Lidar. $K^L_{(k,i)}$ is defined the coordinates of the point in $L_k, i, i \in N_k$ point cloud. Referenced coordinate system is shown by $\{D\}$ and a point coordinate inside this coordinate system is shown by $K^D_{(k,i)}$. Let G be the set of points obtained during a scan by k optical channel. Moreover, the surface roughness metric κ will be;

$$\kappa = \frac{1}{|G|.\left\|K^L_{(k,i)}\right\|} \left\|\sum_{j\in G, j\neq i}(K^L_{(k,i)} - K^L_{(k,j)}\right\| \quad (1)$$

Measured points are sorted within this metric in order to define which ones are edge (maximum values or above the threshold), Γ_k, which ones are surface (minimum values or below the threshold), Δ_k. To find the position difference, that information is used by exploiting Euclidian distances.

The distances from different time interval scans N_k and N_{k+1} is;

$$d_\Gamma = \frac{\left|\left(K^L_{(k+1,i)} - K^L_{(k,j)}\right)\times(K^L_{(k+1,i)} - K^L_{(k,l)})\right|}{K^L_{(k,j)} - K^L_{(k,l)}} \quad (2)$$

where j is the nearest point of edge point $i \in \Gamma_k$, l is the sensed point from the neighbor optical channel $j \in N_{k+1}$, d_Γ is the distance from edge points to the line which is created within (j, l), $j, l \in N_k$ points.

The distance from point to surface will be;

$$d_\Delta = \frac{\left|\begin{matrix}\left(K^L_{(k+1,i)} - K^L_{(k,j)}\right).\left(K^L_{(k,j)} - K^L_{(k,l)}\right) \\ \times(K^L_{(k,j)} - K^L_{(k,m)})\end{matrix}\right|}{\left|\left(K^L_{(k,j)} - K^L_{(k,l)}\right)\times(K^L_{(k,j)} - K^L_{(k,m)})\right|} \quad (3)$$

where j is the nearest point of surface point $i \in \Delta_k$, l is the second nearest point which is sensed from the same optical channel and $j, l \in N_k$. m is the sensed point from the neighbor optical channel, $m \in N_{k+1}$ and d_Δ is the distance from surface points to the surface which is created within (j, l, m), $j, l, m \in N_k$ points.

Let t_σ be the duration of $0 \rightarrow 2\pi$ scan of the 3D Lidar, and t is the moment at investigation of position and localization difference $T^L_\sigma = \left[t_x, t_y, t_z, \theta_x, \theta_y, \theta_z\right]^T$. The position and location difference between $[t_i, t_\sigma]$ is;

$$T^L_{\sigma,i} = \frac{t_i - t_\sigma}{t - t_\sigma} T^L_\sigma \quad (4)$$

16 optical channeled 3D Lidar measures environment in δ_z time steps. So, the rotation and translation terms can be

written as;

$$K^L_{(k,j)_t} = R.K^L_{(k,j)_{t-\delta_z}} + T^L_{\sigma,i} \quad (5)$$

where R is the rotation matrix. In this case, features of edge and surface geometric relationship can be written as functions given below;

$$f_\Gamma\left(K^L_{(k,j)_t}, T^L_{\sigma,i}\right) = d_\Gamma,\ i \in \Gamma_k \quad (6)$$
$$f_\Delta\left(K^L_{(k,j)_t}, T^L_{\sigma,i}\right) = d_\Delta,\qquad i \in \Delta_k$$

Finally, by handling nonlinear optimization method, minimized function for each feature point is obtained;

$$\min(T^L_{\sigma,i} - (J^TJ + \lambda diag(J^TJ))J^Td) \quad (8)$$

where $f\left(T^L_{\sigma,i}\right) = d$ is the nonlinear distance, $J = \delta f/\delta T^L_{\sigma,i}$ and λ is a factor provided by Levenberg-Marquardt method. By minimizing, the distance to zero $T^L_{\sigma,i}$ is found. Also, the georeferenced point cloud, $K^L_{(k,j)_t}$ is obtained.

B. Grid Mapping

Occupancy grid mapping technique uses that information to define the cells of the 2D map is occupied. This technique degrades the whole maps occupation determination to each cell and calculate the state of it separately.

In order to determine the occupancy probability of the cells for the whole map globally, probabilities of each cell is multiplied [13]

$$P\left(\mathrm{M}_{x_t,y_t}, Z_{0:t}\right) = \prod_{x,y} P\left(m_{x_t,y_t}, Z_{0:t}\right) \quad (8)$$

It was desired to handle the environment in 3D since the Octree Mapping technique is used for continuing with height maps. In Octree Mapping technique, environmental volume of the extracted map is divided in cubes named as voxel and for each cube occupation information is written in this mapping technique [12]. In this method, each cube always divided to eight subparts in order to obtain smaller volumes. By using this approach, the smallest volumes information can be reached. So, the octree map method is more sophisticated than the fixed size 3D maps. Equation (1) is also exploited by adding another dimension z to get 3D Octree Map of the environment.

$$P\left(\mathrm{M}_{x_t,y_t,z_t}, Z_{0:t}\right) = \prod_{x,y} P\left(m_{x_t,y_t,z_t}, Z_{0:t}\right) \quad (9)$$

C. Similarity Metrics

For handling the matching problem, similarity measures can be benefited. Probabilistic uncertainty which is known as entropy is the main concept of Shannon's entropy family. Entropy of M can be defined as (3);

$$H(M) = \sum_{i=1}^{d} M_i \ln M_i \quad (10)$$

Similarity measures can be grouped as distinctive families [10]. Kullback-Liebler divergence, Jeffreys and K divergence are the main definitions which are given below;

KL divergence;

$$d_{KL} = \sum_{i=1}^{d} M^h_{d\,i} \ln \frac{M^h_{d\,i}}{M_{b_i}} \quad (11)$$

Jeffreys;

$$d_J = \sum_{i=1}^{d} (M^h_{d\,i} - M^h_{b\,i}) \ln \frac{M^h_{d\,i}}{M^h_{b\,i}} \quad (12)$$

K divergence;

$$d_K = \sum_{i=1}^{d} M^h_{d\,i} \ln \frac{2M^h_{d\,i}}{M^h_{d\,i} + M^h_{b\,i}} \quad (13)$$

where $M^h_d(X)$ is the ground vehicles height map and the $M^h_b(X + p)$ is the aerial vehicles height map with p position and orientation.

After finding the minimum distances by choosing the best p value, the position and orientation difference between aerial and ground maps are found. Finally, the global map of the environment is obtained within matching maps in 3D environment.

IV. Simulation Results

Simulation is done by using height map methods [9] on the complicated scene (Fig. 2) which has different obstacles, objects that cannot be seen form bird-eye view and objects that cannot be seen from ground sensors. Especially trees, structures that have closed top and open four sides and objects have different projection and top view.

Fig. 2 Simulation scene

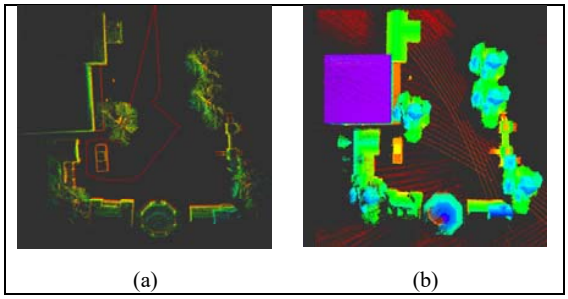

(a) (b)

Fig. 3 Georeferenced point clouds (a) ground vehicle (b) aerial vehicle

Referenced point clouds obtained at the beginning by

ground and aerial vehicles are given in Fig. 3.

Resulted Octree Maps are given in Fig. 4.

We aimed for finding the best map match for our ground vehicles VLP-16 Lidar sensor field of view which is 15° in z direction above the ground. So, we used heights less than 1 meter from the ground. Moreover, the whole area was not investigated for matching the maps. The environment is partitioned to $10m \times 10m$ areas in 2D in order to check the similarities between base and draft map which are obtained respectively by aerial vehicle and ground vehicle as shown in Fig. 5.

Best similarity scores are achieved by K divergence, while KL divergence is very close to that similarity metric. Jeffreys similarity score is almost two times of K divergence.

Within the usage of height values of the cells, maps are merged, and the resulting global occupancy map is obtained (Fig. 6).

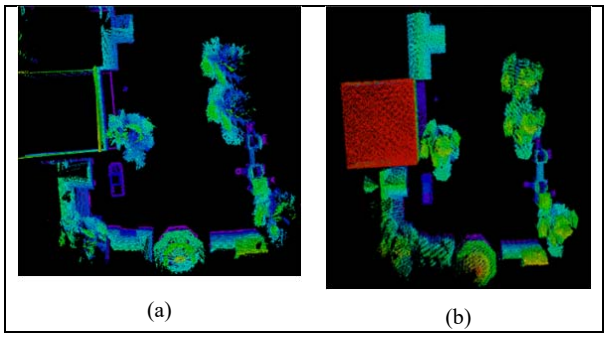

Fig. 4 Octree map of the environment (a) ground vehicle, (b) aerial vehicle

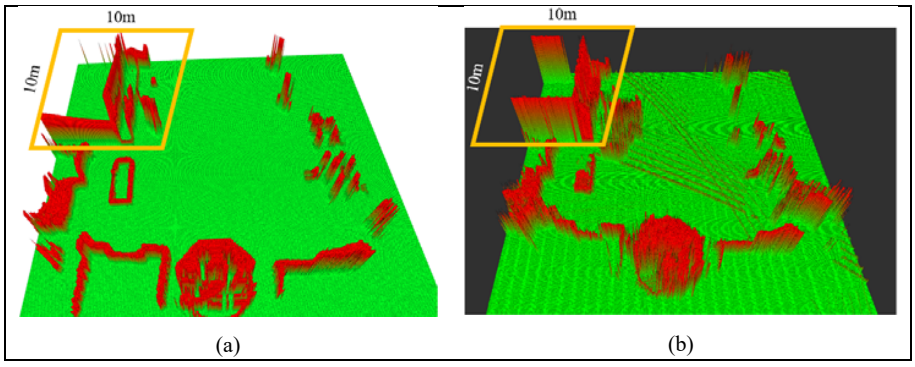

Fig. 5 Matched areas of the maps

Fig. 6 Resulting common global occupancy map of the simulation scene

V. Conclusion

In our specific study, HRT managed to attain a common map with the Shannon's entropy theoretic similarity metrics. Also, localization of the robots and the global occupancy grid map is obtained.

In future work, we aim to continue with the experimental studies in order to understand the real world results. Moreover, environment can be extra complex for more compelling studies.

Acknowledgment

This work is supported by the Scientific and Technological Research Council of Turkey (TÜBİTAK) under grant number 116E178.

References

[1] L. E. Parker, B. Kannan, F. T. F. Tang, and M. Bailey, "Tightly-coupled navigation assistance in heterogeneous multi-robot teams," *2004 IEEE/RSJ Int. Conf. Intell. Robot. Syst. (IEEE Cat. No.04CH37566)*, vol. 1, pp. 1016–1022, 2004.

[2] M. Hofmeister, M. Kronfeld, and A. Zell, "Cooperative visual mapping in a heterogeneous team of mobile robots," *Proc. - IEEE Int. Conf. Robot. Autom.*, pp. 1491–1496, 2011.

[3] T. Bailey, M. Bryson, H. Mu, J. Vial, L. McCalman, and H. Durrant-Whyte, "Decentralised cooperative localisation for heterogeneous teams of mobile robots," *Proc. - IEEE Int. Conf. Robot. Autom.*, pp. 2859–2865, 2011.

[4] M. Langerwisch, T. Wittmann, S. Thamke, T. Remmersmann, A. Tiderko, and B. Wagner, "Heterogeneous teams of unmanned ground and aerial robots for reconnaissance and surveillance-a field experiment," *Safety, Secur. Rescue Robot. (SSRR), 2013 IEEE Int. Symp.*, pp. 1–6, 2013.

[5] Y. Ktiri and M. Inaba, "A framework for multiple heterogeneous robots exploration using laser data and MARG sensor," *2012 IEEE/SICE Int. Symp. Syst. Integr. SII 2012*, pp. 635–640, 2012.

[6] A. Husain *et al.*, "Mapping planetary caves with an autonomous, heterogeneous robot team," *IEEE Aerosp. Conf. Proc.*, 2013.

[7] C. Forster, M. Pizzoli, and D. Scaramuzza, "Air-ground localization and map augmentation using monocular dense reconstruction," *IEEE Int. Conf. Intell. Robot. Syst.*, pp. 3971–3978, 2013.
[8] L. Kneip, M. Chli, and R. Y. Siegwart, "Robust Real-Time Visual Odometry with a Single Camera and an IMU.," *Bmvc*, p. 16.1-16.11, 2011.
[9] R. Kaeslin *et al.*, "Collaborative Localization of Aerial and Ground Robots through Elevation Maps," *IEEE Int. Symp. Safety, Secur. Map/Collaborative_Navigation_for_Flying_and_Walking_Robots_Marco_Hutter_2016.pdfy Rescue Robot.*, 2016.
[10] S. Cha, "Comprehensive Survey on Distance / Similarity Measures between Probability Density Functions," vol. 1, no. 4, 2007.
[11] J. Zhang and S. Singh, "LOAM: Lidar Odometry and Mapping in Real-time," 2014.
[12] A. Hornung, K. M. Wurm, M. Bennewitz, C. Stachniss, and W. Burgard, "OctoMap: An efficient probabilistic 3D mapping framework based on octrees," *Auton. Robots*, vol. 34, no. 3, pp. 189–206, 2013.
[13] M. Santana, K. R. T. Aires, and R. M. S. Veras, "An Approach for 2D Visual Occupancy Grid Map Using Monocular Vision," vol. 281, pp. 175–191, 2011.